Buckling Analysis of Stiffened and Unstiffened Laminated Composite Plates

Dr. Adnan Naji Jameel
Professor
University of Baghdad
College of Engineering
Mechanical Engineering Dep.
adnanaji2004@yahoo.com

Dr. louay Sabah yousuf
Assistant Professor
University of Baghdad
College of Engineering
Mechanical Engineering Dep.
louaysabah79@yahoo.com

Eng.Ahmed Mahdi Salih
Researcher
University of Baghdad
College of Engineering
Mechanical Engineering Dep.
flightstar8888@yahoo.com

ABSTRACT

The present study focused mainly on the analysis of stiffened and unstiffened composite laminated plates subjected to buckling load. Analytical, numerical and experimental analysis for different cases has been considered. The experimental investigation is to manufacture the laminates and to find mechanical properties of glass-polyester such as longitudinal, transverse young modulus, shear modulus. The compressive test was carried to find the critical buckling load of plate. The design parameters of the laminates such as aspect ratio, thickness ratio, boundary conditions and number of stiffeners were investigated using high order shear deformation theory (HOST) and Finite element coded by ANSYS .The main conclusion was the buckling load could increase and decrease depending on the boundary conditions, thickness ratio, and, the aspect ratio and number of stiffeners of the plate.

Keywords: composite laminated plate, glass-polyester, bucking load, high order shear deformation, stiffened and unstiffened plate.

تحليل الصفائح المركبة المقواة والغير مقواة تحت تأثير حمل الانبعاج

د. عدنان ناجي جميل
أستاذ
جامعة بغداد \ كلية الهندسة

د. لؤي صباح يوسف
أستاذ مساعد
جامعة بغداد \ كلية الهندسة

المهندس احمد مهدي صالح
باحث
جامعة بغداد \ كلية الهندسة

الخلاصة

هذه الدراسة ركزت بشكل رئيسي على تحليل الصفائح المركبة المقواة والغير مقواة المعرضة لحمل الانبعاج.وتم التحليل النظري،التحليل العددي والعملي لمختلف الحالات.في الجانب العملي تم تصنيع الصفائح المركبة المصنوعة من الالياف الزجاجية والبوليستر لايجاد الخواص الميكانيكية مثل معامل يونك الطولي والعرضي ومعامل القص.تم عمل اختبار الانضغاط للعثور على القيمة الحرجة لحمل الانبعاج للصفيحة. كما تم بحث عناصر تصميم شرائح مثل نسبةالعرض إلى الارتفاع،ونسبة سماكة وشروط الحدية وعدد المقويات باستخدام النظرية تشوه القص الدرجة العالية و طريقة العناصر المحددة المبرمجة باستخدام برنامج ANSYS.وكان الاستنتاج الرئيسي ان قيمة حمل الانبعاج يمكن ان يقل او يزيد تبعا لشروط الحدية،ونسبة سماكة،ونسبةالعرض إلى الارتفاع لوحة وعدد المقويات للبيليتة.

الكلمات الرئيسية: صفائح مركبة,ألياف زجاجية , حمل الانبعاج , نظرية تشوه القص الدرجة العالية للصفائح الطباقية,الصفائح المقواة وغير المقواة .

1. INTRODUCTION

1.1 General

During the last decades, needs for *composite materials* which contain two or more types of materials mixed together homogenously have appeared.

Composite materials have many advantages such as high strength with low weight compared with traditional engineering materials; furthermore, their properties can be controlled during mixing of their components to meet the suitable design requirements.

When a flat plate is subjected to low in-plane compressive loads, it remains flat and is in equilibrium condition. As the magnitude of the in-plane load increases, however, the equilibrium configuration of the plate is eventually changed to a non-flat configuration and the plate becomes unstable and begins to deflect to the middle portion. **, Reddy J.N. 2004.**

Many researches had studied buckling analysis of stiffened and unstiffened plate.

Guedes Soares C. and **Gordo J. M.1997,** performed of three methods to design stiffened panels under predominantly in plane uniaxial compressive loading is compared by referring to numerical and experimental results.

Satish Kumar Y.V., Madhujit Mukhopadhyay 1999, presented the basic plate element is a combination of Allman's plane stress triangular element and a Discrete Kirchhoff-Mindlin plate bending element. The element includes transverse shear effects. The model accommodates any number of arbitrarily oriented stiffeners within the plate element and eliminates constraints on the mesh division of the plate.

Rikards R. etal 2001, concentrated on the development of triangular finite element for buckling and vibration analysis of laminated composite stiffened shells. For the laminated shell, an equivalent layer shell theory is employed. The first-order shear deformation theory including extension of the normal line is used. In order to take into account a non-homogeneous distribution of the transverse shear stresses a correction of transverse shear stiffness is employed. Results of vibration and buckling analysis of stiffened plates and shells are discussed.

Samuel Kidane2002, investigated buckling loads of stiffened composite cylinders under uniaxial loading condition by using analytical and experimental approaches. The stiffness contributions of the stiffeners are computed by analyzing the moment and force effect of the stiffener on a unit cell. Then the equivalent stiffness of the stiffener/shell panel is computed by superimposing the stiffness contribution of the stiffeners and the shell. Once the equivalent stiffness parameters are determined for the whole panel, the buckling load is calculated using the energy method.

Aseel Jasim Mohammed Al-Hassani 2005, investigated the vibration characteristic of composite plates with and without holes ,manufactures of fiber glass+ polyester in the presence of steel layers reinforcement , stiffeners subjected to various load conditions and constraints (simply supported and clamped).

An experimental programmed was also conducted in order to obtain the material properties of the used plates and study the plate behavior under static load and measuring the strain and deflection from which the structures are obtained and compared with the numerical results.

Akl W. etal 2008, selected the orientation angles of stiffeners arranged in the form of isogrid configuration over a flat plate to optimize the static and dynamic characteristics of these plates/stiffeners assemblies. The static characteristics are optimized by maximizing the critical buckling loads of the isogrid plate, while the dynamic characteristics are optimized by maximizing multiple natural frequencies of the stiffened plate.

Tran Ich Thinh and Tran Huu Quoc2010, studied free vibration and bending failure of laminated stiffened glass fiber/polyester composite plates with laminated open section (rectangular or T-shaped) and closed section (hat shaped) of stiffeners by finite element method and experiment. The results calculated by computational model for above plates under different boundary conditions are in good agreement with experiments. The failure problems of these stiffened glass fiber/polyester composite plates are also investigated.

Hasanain Ibrahim Nsaif 2011, investigated Buckling analysis of composite laminates for critical thermal and mechanical loads. The analytical investigation involved certain mathematical preliminaries, a study of equations of orthotropic elasticity for classical laminated plate theory (CLPT), higher order shear deformation plate theory (HSDT), and numerical analysis (Finite element method).

The present work is focused on how to derive the analytical solution of critical bucking load for stiffened and unstiffened composite laminated plates by high order shear deformation theory by applied different type of boundary condition on the symmetric cross-ply composite laminated plates using Levy solution .Mechanical properties, buckling load for composite plate made from (glass-polyester) with fiber volume fraction (0.3) are determined experimentally.

Also Finite element coded by ANSYS12.1used to find critical buckling load of stiffened and unstiffened composite laminate plate.

2. ANALYTICAL SOLUTION (HIGHER ORDER SHEAR DEFORMATION PLATE THEORY)

2.1. Unstiffened Laminated Plate

2.1.1 Displacement

High order shear deformation plate theory (HSDT) based on assuming the straight line perpendicular to the mid surface before deformation become curve line after deformation, **Reddy, J.N. 2004**.

$$u(x,y,z,t)=u_o(x,y,t)+z\emptyset_x(x,y,t)-\frac{4}{3h^2}z^3\left(\emptyset_x+\frac{\partial w_0}{\partial x}\right) \quad \textbf{(1. a)}$$

$$v(x,y,z,t)=v_o(x,y,t)+z\emptyset_y(x,y,t)-\frac{4}{3h^2}z^3\left(\emptyset_y+\frac{\partial w_0}{\partial y}\right) \quad \textbf{(1. b)}$$

$$w(x,y,z,t)=w_o(x,y,t) \quad \textbf{(1. c)}$$

2.1.2 Stress and strain

The total strains can be written as follows

$$\begin{Bmatrix}\varepsilon_{xx}\\ \varepsilon_{yy}\\ \gamma_{xy}\end{Bmatrix}=\begin{Bmatrix}\varepsilon_{xx}^{(0)}\\ \varepsilon_{yy}^{(0)}\\ \gamma_{xy}^{(0)}\end{Bmatrix}+z\begin{Bmatrix}\varepsilon_{xx}^{(1)}\\ \varepsilon_{yy}^{(1)}\\ \gamma_{xy}^{(1)}\end{Bmatrix}+z^3\begin{Bmatrix}\varepsilon_{xx}^{(3)}\\ \varepsilon_{yy}^{(3)}\\ \gamma_{xy}^{(3)}\end{Bmatrix} \quad \textbf{(2.a)}$$

$$\begin{Bmatrix}\gamma_{yz}\\ \gamma_{xz}\end{Bmatrix}=\begin{Bmatrix}\gamma_{yz}^{(0)}\\ \gamma_{xz}^{(0)}\end{Bmatrix}+z\begin{Bmatrix}\gamma_{yz}^{(1)}\\ \gamma_{xz}^{(1)}\end{Bmatrix}+z^2\begin{Bmatrix}\gamma_{yz}^{(2)}\\ \gamma_{xz}^{(2)}\end{Bmatrix} \quad \textbf{(2.b)}$$

The transformed stress-strain relations of an orthotropic lamina in a plane state of stress are; for $\bar{Q}_{ij}$ see ,**Reddy J.N. 2004**.

$$\begin{Bmatrix}\sigma_{xx}\\ \sigma_{yy}\\ \sigma_{xy}\end{Bmatrix}_k = \begin{bmatrix}\bar{Q}_{11} & \bar{Q}_{12} & \bar{Q}_{16}\\ \bar{Q}_{12} & \bar{Q}_{22} & \bar{Q}_{26}\\ \bar{Q}_{16} & \bar{Q}_{26} & \bar{Q}_{66}\end{bmatrix}_k \begin{Bmatrix}\varepsilon_{xx}\\ \varepsilon_{yy}\\ \gamma_{xy}\end{Bmatrix} \quad \textbf{(3.a)}$$

$$\begin{Bmatrix}\sigma_{yz}\\ \sigma_{xz}\end{Bmatrix}_k = \begin{bmatrix}\bar{Q}_{44} & \bar{Q}_{45}\\ \bar{Q}_{45} & \bar{Q}_{55}\end{bmatrix} \begin{Bmatrix}\gamma_{yz}\\ \gamma_{xz}\end{Bmatrix} \quad \textbf{(3.b)}$$

The result stress Nxx, Nyy and Nxy, Mxx,Myy and Mxy , shear force Qxz, Qyz, Rxz, Ryz , and the higher order stress resultants Pxx, Pyy and Pxy acting on a laminate are obtained by integration of the stress in each layer or lamina through the laminate thickness. Knowing the stress in terms of the displacement, the stress resultants Nxx, Nyy, Nxy, Mxx, Myy, Mxy, Qxz, Qyz, Pxx, Pyy, Pxy, Rx and Ry can be obtained .

The inplane force resultants are defined as

$$\begin{Bmatrix}\mathrm{N_{xx}}\\ \mathrm{N_{yy}}\\ \mathrm{N_{xy}}\end{Bmatrix} = \sum_{r=1}^{N} \int_{z_k}^{z_{k+1}} \begin{Bmatrix}\sigma_{xx}\\ \sigma_{yy}\\ \sigma_{xy}\end{Bmatrix}_k dz \quad \textbf{(4.a)}$$

Whereσ_x , σ_y and σ_{xy} are normal and shear stress.

$$\begin{Bmatrix}N_{xx}\\ N_{yy}\\ N_{xy}\end{Bmatrix} = \begin{bmatrix}A_{11} & A_{12} & A_{16}\\ A_{12} & A_{22} & A_{26}\\ A_{16} & A_{26} & A_{66}\end{bmatrix} \begin{Bmatrix}\varepsilon^0_{xx}\\ \varepsilon^0_{yy}\\ \gamma^0_{xy}\end{Bmatrix} + \begin{bmatrix}B_{11} & B_{12} & B_{16}\\ B_{12} & B_{22} & B_{26}\\ B_{16} & B_{26} & B_{66}\end{bmatrix} \begin{Bmatrix}\varepsilon^1_{xx}\\ \varepsilon^1_{yy}\\ \gamma^1_{xy}\end{Bmatrix} - c_1 \begin{bmatrix}E_{11} & E_{12} & E_{16}\\ E_{12} & E_{22} & E_{26}\\ E_{16} & E_{26} & E_{66}\end{bmatrix} \begin{Bmatrix}\varepsilon^{(3)}_{xx}\\ \varepsilon^{(3)}_{yy}\\ \gamma^{(3)}_{xy}\end{Bmatrix} \quad \textbf{(4.b)}$$

$$\begin{Bmatrix}M_{xx}\\ M_{yy}\\ M_{xy}\end{Bmatrix} = \sum_{r=1}^{N} \int_{z_k}^{z_{k+1}} \begin{Bmatrix}\sigma_{xx}\\ \sigma_{yy}\\ \sigma_{xy}\end{Bmatrix}_k z\, dz \quad \textbf{(5.a)}$$

$$\begin{Bmatrix}M_{xx}\\ M_{yy}\\ M_{xy}\end{Bmatrix} = \begin{bmatrix}B_{11} & B_{12} & B_{16}\\ B_{12} & B_{22} & B_{26}\\ B_{16} & B_{26} & B_{66}\end{bmatrix} \begin{Bmatrix}\varepsilon^0_{xx}\\ \varepsilon^0_{yy}\\ \gamma^0_{xy}\end{Bmatrix} + \begin{bmatrix}D_{11} & D_{12} & D_{16}\\ D_{12} & D_{22} & D_{26}\\ D_{16} & D_{26} & D_{66}\end{bmatrix} \begin{Bmatrix}\varepsilon^1_{xx}\\ \varepsilon^1_{yy}\\ \gamma^1_{xy}\end{Bmatrix} - c_1 \begin{bmatrix}F_{11} & F_{12} & F_{16}\\ F_{12} & F_{22} & F_{26}\\ F_{16} & F_{26} & F_{66}\end{bmatrix} \begin{Bmatrix}\varepsilon^{(3)}_{xx}\\ \varepsilon^{(3)}_{yy}\\ \gamma^{(3)}_{xy}\end{Bmatrix} \quad \textbf{(5.b)}$$

$$\begin{Bmatrix}\mathrm{P_{xx}}\\ \mathrm{P_{yy}}\\ \mathrm{P_{xy}}\end{Bmatrix} = \sum_{k=1}^{N} \int_{z_k}^{z_{k+1}} \begin{Bmatrix}\sigma_x\\ \sigma_y\\ \sigma_{xy}\end{Bmatrix}_k z^3\, dz \quad \textbf{(6.a)}$$

$$\begin{Bmatrix}P_{xx}\\ P_{yy}\\ P_{xy}\end{Bmatrix} = \begin{bmatrix}E_{11} & E_{12} & E_{16}\\ E_{12} & E_{22} & E_{26}\\ E_{16} & E_{26} & E_{66}\end{bmatrix} \begin{Bmatrix}\varepsilon^0_{xx}\\ \varepsilon^0_{yy}\\ \gamma^0_{xy}\end{Bmatrix} + \begin{bmatrix}F_{11} & F_{12} & F_{16}\\ F_{12} & F_{22} & F_{26}\\ F_{16} & F_{26} & F_{66}\end{bmatrix} \begin{Bmatrix}\varepsilon^1_{xx}\\ \varepsilon^1_{yy}\\ \gamma^1_{xy}\end{Bmatrix} - c_1 \begin{bmatrix}H_{11} & H_{12} & H_{16}\\ H_{12} & H_{22} & H_{26}\\ H_{16} & H_{26} & H_{66}\end{bmatrix} \begin{Bmatrix}\varepsilon^{(3)}_{xx}\\ \varepsilon^{(3)}_{yy}\\ \gamma^{(3)}_{xy}\end{Bmatrix} \quad \textbf{(6.b)}$$

$$\begin{Bmatrix} Q_{yz} \\ Q_{xz} \end{Bmatrix} = \int_{-h/2}^{h/2} \begin{Bmatrix} \sigma_{yz} \\ \sigma_{xz} \end{Bmatrix}_k dz \quad \textbf{(7.a)}$$

$$\begin{Bmatrix} Q_{yz} \\ Q_{xz} \end{Bmatrix} = \begin{bmatrix} A_{44} & A_{45} \\ A_{45} & A_{55} \end{bmatrix} \begin{Bmatrix} \gamma_{yz}^{(0)} \\ \gamma_{xz}^{(0)} \end{Bmatrix} - c_2 \begin{bmatrix} D_{44} & D_{45} \\ D_{45} & D_{55} \end{bmatrix} \begin{Bmatrix} \gamma_{yz}^{(2)} \\ \gamma_{xz}^{(2)} \end{Bmatrix} \quad \textbf{(7.b)}$$

$$\begin{Bmatrix} R_{yz} \\ R_{xz} \end{Bmatrix} = \int_{-h/2}^{h/2} \begin{Bmatrix} \sigma_{yz} \\ \sigma_{xz} \end{Bmatrix}_k z^2 \, dz \quad \textbf{(8.a)}$$

$$\begin{Bmatrix} R_{yz} \\ R_{xz} \end{Bmatrix} = \begin{bmatrix} D_{44} & D_{45} \\ D_{45} & D_{55} \end{bmatrix} \begin{Bmatrix} \gamma_{yz}^{(0)} \\ \gamma_{xz}^{(0)} \end{Bmatrix} - c_2 \begin{bmatrix} F_{44} & F_{45} \\ F_{45} & F_{55} \end{bmatrix} \begin{Bmatrix} \gamma_{yz}^{(2)} \\ \gamma_{xz}^{(2)} \end{Bmatrix} \quad \textbf{(8.b)}$$

Where

$$A_{ij}, B_{ij}, D_{ij}, E_{ij}, F_{ij}, H_{ij} = \sum_{k=1}^{N} \int_{z_k}^{z_{k+1}} \bar{Q}_{ij}^{(k)} (1, z, z^2, z^3, z^4, z^6) \, dz \quad \textbf{(9)}$$

2.1.3 Equation of motion

The Euler-Lagrange equations are obtained by setting the coefficient of δu_0, δv_0, δw_0, $\delta \emptyset_x$, $\delta \emptyset_y$ to zero separately

$$\frac{\partial N_{xx}}{\partial x} + \frac{\partial N_{xy}}{\partial y} = 0 \quad \textbf{(10.a)}$$

$$\frac{\partial N_{xy}}{\partial x} + \frac{\partial N_{yy}}{\partial y} = 0 \quad \textbf{(10.b)}$$

$$\frac{\partial Q_x}{\partial x} - c_2 \frac{\partial R_x}{\partial x} + \frac{\partial Q_y}{\partial y} - c_2 \frac{\partial R_y}{\partial y} + c_1 \left(\frac{\partial^2 P_{xx}}{\partial x^2} + 2 \frac{\partial^2 P_{xy}}{\partial x \, \partial y} + \frac{\partial^2 P_{yy}}{\partial y^2} \right) + \hat{N}_{xx} \frac{\partial^2 w}{\partial x^2} + \hat{N}_{yy} \frac{\partial^2 w}{\partial y^2} + 2 \hat{N}_{xy} \frac{\partial^2 w}{\partial x \partial y} = 0 \quad \textbf{(10.c)}$$

$$\frac{\partial M_{xx}}{\partial x} - c_1 \frac{\partial P_{xx}}{\partial x} + \frac{\partial M_{xy}}{\partial y} - c_1 \frac{\partial P_{xy}}{\partial y} - Q_x + c_2 R_x = 0 \quad \textbf{(10.d)}$$

$$\frac{\partial M_{xy}}{\partial x} - c_1 \frac{\partial P_{xy}}{\partial x} + \frac{\partial M_{yy}}{\partial y} - c_1 \frac{\partial P_{yy}}{\partial y} - Q_y + c_2 R_y = 0 \quad \textbf{(10.e)}$$

These equations of motion (10a-e) can be expressed in terms of displacements **(δu_0, δv_0, δw_0, , $\boldsymbol{\delta \emptyset_x}$, $\boldsymbol{\delta \emptyset_y}$)**by substituting the forces results from eqs. (4,5,6,7,8) into eq. (10.a) to (10.e) and get partial differential equations, then the analytical solution done by levy method as derived in[9].

2.2 Stiffened Laminated Plate

2.2.1 Stress and strain

The displacements field of laminated plate are as given in Eqs (1(a-c)). The distribution of the normal strains over the depth of the stiffened plate is shown in **Fig. (1),** [10]

Then, the stress strain relations for laminated plate are as in Eqs. (3,a-b) and the stress strain relations for stiffeners can be defined as:

$\sigma_{xx})st = E_x^{st} . \varepsilon_{xx}$, $\sigma_{yy})st = E_y^{st} . \varepsilon_{yy}$

$\tau_{xy})\, st=0$, $\tau_{yz})\, st=G_y^{st} . \gamma_{yz}$,

$\tau_{xz})\, st=G_x^{st} . \gamma_{xz}$ **(11)**

Where,$G_x^{st}$and G_y^{st} are shear modules of elasticity of stiffeners in x and y directions , respectively.
The force and moment relation for stiffened plate are:

$$\begin{bmatrix} N \\ M \\ P \end{bmatrix} = \begin{bmatrix} N \\ M \\ P \end{bmatrix}_{unst} + \begin{bmatrix} N \\ M \\ P \end{bmatrix}_{st} ,$$

$$And, \quad \begin{bmatrix} Q \\ R \end{bmatrix} = \begin{bmatrix} Q \\ R \end{bmatrix}_{unst} + \begin{bmatrix} Q \\ R \end{bmatrix}_{st} \quad \textbf{(12)}$$

Where, $\begin{bmatrix} N \\ M \\ P \end{bmatrix}_{unst} \; and \; \begin{bmatrix} Q \\ R \end{bmatrix}_{unst}$ are force and moment relations for laminated plate as in Eqs. (4, 5, 6, 7, 8(a-b)).

And $\begin{bmatrix} N \\ M \\ P \end{bmatrix}_{st} \; and \; \begin{bmatrix} Q \\ R \end{bmatrix}_{st}$ are forces and moment relations for stiffeners can be defined as:

$$N_{xx})st. = \int_{Zi-1)x^{st}}^{Zi)x^{st}} \sigma_x)st \,.\frac{tx}{bx} \,.dZ$$

$$N_{yy})st. = \int_{Zi-1)y^{st}}^{Zi)y^{st}} \sigma_y)st.\frac{ty}{by} \,.dZ, N_{xy})st = 0$$

$$M_{xx})st. = \int_{Zi-1)x^{st}}^{Zi)x^{st}} \sigma_x)st \,.\frac{tx}{bx} \,.Z.dZ$$

$$M_{yy})st. = \int_{Zi-1)y^{st}}^{Zi)y^{st}} \sigma_y)st.\frac{ty}{by} \,.Z.dZ, M_{xy})st = 0$$

$$P_x)st. = \int_{Zi-1)x^{st}}^{Zi)x^{st}} \sigma_x)st \,.\frac{tx}{bx} \,.Z^3 \,.dZ \quad \textbf{(13)}$$

$$P_y)st. = \int_{Zi-1)y^{st}}^{Zi)y^{st}} \sigma_y)st.\frac{ty}{by} \,.Z^3 \,.dZ,$$

$$P_{xy})st = 0$$

Where,
$Zi)x^{st}$, $Zi-1)x^{st}$, $Zi)y^{st}$,
$Zi-1)y^{st}$, t_x , b_x , t_y , b_y as shown in **Fig.2** or, Eq. (13) can be written as:

$$\begin{bmatrix} N_{xx} \\ N_{yy} \\ M_{xx} \\ M_{yy} \\ P_x \\ P_y \end{bmatrix}_{st} = \begin{bmatrix} A_{11}^{st} & 0 \\ 0 & A_{22}^{st} \\ B_{11}^{st} & 0 \\ 0 & B_{22}^{st} \\ E_{11}^{st} & 0 \\ 0 & E_{22}^{st} \end{bmatrix} \begin{bmatrix} \varepsilon_{xx} \\ \varepsilon_{yy} \end{bmatrix} \quad (\textbf{14})$$

Where,

$$(A_{11}^{st}, B_{22}^{st}, D_{11}^{st}, E_{11}^{st}) = \int_{Zi-1)x^{st}}^{Zi)x^{st}} \frac{tx}{bx} \,.Ex^{st}.(1, Z, Z^2, Z^3).dZ \quad \textbf{(15a)}$$

$$(A_{11}^{st}, B_{22}^{st}, D_{11}^{st}, E_{11}^{st}) = \int_{Zi-1)y^{st}}^{Zi)y^{st}} \frac{ty}{by} \,.Ey^{st}.(1, Z, Z^2, Z^3).dZ \quad \textbf{(15b)}$$

And, $\begin{bmatrix} Q \\ R \end{bmatrix}_{st}$ can be defined as in equations:

$$\left.\begin{aligned} Q_{yz})st &= \int_{Zi-1)y^{st}}^{Zi)y^{st}} \gamma_{yz} \cdot Gy^{st} \cdot \frac{ty}{by} \cdot dZ \\ Q_{xz})st &= \int_{Zi-1)x^{st}}^{Zi)x^{st}} \gamma_{xz} \cdot Gx^{st} \cdot \frac{tx}{bx} \cdot dZ \\ R_{yz})st &= \int_{Zi-1)y^{st}}^{Zi)y^{st}} \gamma_{yz} \cdot Gy^{st} \cdot \frac{ty}{by} \cdot Z^2 \cdot dZ \\ R_{xz})st &= \int_{Zi-1)x^{st}}^{Zi)x^{st}} \gamma_{xz} \cdot Gx^{st} \cdot \frac{tx}{bx} \cdot Z^2 \cdot dZ \end{aligned}\right\} \quad \textbf{(16a)}$$

Or, equation (16a) can be written as:

$$\begin{bmatrix} Q_{yz} \\ Q_{xz} \\ R_{yz} \\ R_{xz} \end{bmatrix} st = \begin{bmatrix} A_{44}^{st} & 0 \\ 0 & A_{55}^{st} \\ D_{44}^{st} & 0 \\ 0 & D_{55}^{st} \end{bmatrix} \begin{bmatrix} \gamma_{yz} \\ \gamma_{xz} \end{bmatrix} \quad \textbf{(16b)}$$

Where,

$$A_{44}^{st} = \int_{Zi-1)y^{st}}^{Zi)y^{st}} Gy^{st} \cdot \frac{ty}{by} \cdot dZ,$$

$$A_{55}^{st} = \int_{\substack{Zi-1)x^{st} \\ Zi)y^{st}}} Gx^{st} \cdot \frac{tx}{bx} \cdot dZ$$

$$D_{44}^{st} = \int_{\substack{Zi-1)y^{st} \\ Zi)x^{st}}} Gy^{st} \cdot \frac{ty}{by} \cdot Z^2 \cdot dZ$$

$$D_{55}^{st} = \int_{Zi-1)x^{st}} Gx^{st} \cdot \frac{tx}{bx} \cdot Z^2 \cdot dZ$$

2.2.2 Equations of motion

The refined analysis of such a plate, the governing differential equations are expressed in terms of the displacements, u, v, and w of the middle surface of the plate in the directions x, y, and z, respectively. The displacements at any point are related to those at the middle surface.

3. NUMERICAL ANALYSIS

3.1 Element Selection and Modeling

An element called shell281 as shown in **Fig. 3.** Is selected for unstiffened plate which is suitable for analyzing thin to moderately thick shell structures. The element has eight nodes with six degrees of freedom at each node: translations in the x, y, and z axes, and rotations about the x, y, and z axes. It may be used for layered applications for modeling composite shells. It includes the effects of transverse shear deformation.

Finite element method has been employed to analyze natural frequency and dynamic response. The model was developed in ANSYS 12.1using the 121 quadrate elements (i.e. there are 11 elements in the axial direction and 11 along the width) which means (4416 DOF). Convergence study is the reason for choosing the particular mesh used in this study. The global x coordinate is directed along the width of the plate, while the global y coordinate is directed along the length and

the global z direction corresponds to the thickness direction and taken to be the outward normal of the plate surface. for stiffened plate, the element used is solid-shell 190. SOLSH190 is used for simulating shell structures with a wide range of thickness (from thin to moderately thick) and for stiffened plate. The element possesses the continuum solid element topology and features eight-node connectivity with three degrees of freedom at each node: translations in the nodal x, y, and z directions. And adding degree of freedom rotation on x ,y and z for the present solution by command adding degree of freedom. Thus, connecting SOLSH190 with other continuum elements requires no extra efforts. A degenerate prism option is available, but should only be used as filler elements in mesh generation. The element has plasticity, creep, large deflection, and large strain capabilities. SOLSH190 can use for layered applications such as modeling laminated shells or sandwich construction. . Accuracy in modeling composite shells is governed by the first-order shear-deformation theory (also known as Mindlin-Reissner shell theory).

3.2Verification Case Studies

In the present study, Series of preselected cases are modeled to verify the accuracy of the method of analysis. The results are compared to analytical solution (Levy) and numerical solution (Finite element method).see **Table 1** and **Table 2** for unstiffened plate, and **Table 3** for stiffened plate**.** From these results, it is obvious that the methods of solution gives better results for both analytical and numerical solution.

4. EXPERIMENTAL WORK

In the present work, three- purposes were investigated. First, to outline the general steps to design and fabricate the rectangular test models from fiber (E-glass) and polyester resin to form laminate composite materials. Second, the manufactured models are then used to evaluate the mechanical properties (E_1, E_2, G_{12}) of unidirectional composite material. Third, compressive test to find buckling load of cross ply laminate plate.

4.1Tensile Test

Each laminate was oriented in longitudinal, transverse and 45° angle relative to designated 0° direction to determine the engineering parameters E_1, E_2, G_{12}. Tensile test specimen includes standard geometry according to ASTM (D3039/D03039M); and the mechanical properties for glass-polyester which obtained from tensile test as shown in **Table 4.**

4.2 Buckling Test

In this study, buckling load of laminated plate (stiffened and un-stiffened) determined analytically, numerically and experimentally. The laminated plate length was 200 mm. the width and thickness of it are 100 mm and 4 mm respectively.

For stiffened plate the same dimensions of the un-stiffened plate except with the use of (stiffeners with width of 6mm, two specimen one of them with one stiffener and the other with two). With stiffeners depth 4mm, length of 200mm and the lamination angle for all stiffeners was 0° . The mechanical properties for glass-polyester are obtained from tensile test as shown in **Table 4.**

The specimen was loaded in axial compression (vertical direction) using tensile test machine of 200 KN capacity as shown in **Fig. 4**. the specimen was simply supported by two ends and kept free at the other two ends. The specimen was loaded slowly until buckling. The experimental set up has shown in **Figs. 5a-c)** for three cases. (Un-stiffened and stiffened with one stiffener and with two stiffeners)

Simply supported boundary conditions were simulated along the top and bottom edges. For axial loading, the test specimen was placed between two extremely stiff machine heads of which the lower one was fixed during the test, whereas the upper head was moved downwards by servo hydraulic cylinder. The laminated plate was loaded at constant cross-head speed of 5 mm/min.

The buckling load is determined from the load-displacement curve. The vertical displacement is plotted on the x-axis in (mm) and the load was plotted on the y-axis in (KN).

5. RESULTS AND DISCUSSION

5.1 Experimental R%esults

The critical buckling load is shown in **Tables 5 and 6** for un-stiffened and stiffened plate respectively. Maximum error between analytical and experimental is (3.925%) in case 0/90/90/0 un-stiffened plate and maximum error between numerical and experimental is 8.27% for the same case. For stiffened plate (pate with one stiffener) maximum error between analytical and experimental is (1.762%) in case 0/90/0 stiffened plate and maximum error between numerical and experimental is7.72% for the same case. For stiffened plate (pate with two stiffeners) maximum error between analytical and experimental is (2.608%) in case 0/90 stiffened plate and maximum error between numerical and experimental is5.47% for the same case.

5.2Theoretical Results Contain (analytical and numerical (ANSYS))

In this section the effect of different parameter on critical buckling load are discussed such as boundary conditions aspect ratio, thickness ratio, number of stiffeners and stiffener depth ratio for cross ply composite laminate plate. This result found by analytical method using HSDT with Levy method and numerically using ANSYS 12.1 program.

5.2.1 Boundary conditions

From the results listed in **Table 7** it can be observed that the boundary conditions always affect on the buckling load. It′s worth mentioning that the critical buckling load in SCSC and SSSC for cross ply and CSCS are higher than other cases because of B.C′S. effect.

5.2.2 Aspect ratio

For unstiffened plate, **Fig. 6** shows that in SSSF and SFSF the buckling load decreases when a/b increases with high percentage reaches to 72.51% and 74.45% in SSSF and SFSF respectively. On the other hand in SCSC the buckling load decreases with small percentage reaches to 11.569% when a/b varies from 0.5 to 1.5, Then, it′s increases when a/b varies from 1.5 to 2. The maximum buckling load in SCSC is at a/b=0.5. While the minimum is at a/b=1.5.

Fig.7 shows that in un stiffened plate and plate with one stiffener the buckling load decreases when a/b increase with high percentage reaches to 67.383% and 57.878% in un stiffened plate and plate with one stiffener respectively. On the other hand in plate with two stiffeners the buckling load decreases with percentage reaches to 12.204%, It′s worth mentioning the buckling load in plate with two stiffeners is higher than other cases because of the number of stiffener effect with percentages (78.4% with plate with one stiffener and 88.19% with plate without stiffener when a/b=1).

5.2.3 Thickness ratio

In **Fig. 8,** for unstiffened plate the buckling loads increase when thickness ratio increases. It can be observed that the buckling load is increased with high percentage when b/h varies from 10 to 20. Then, this percentage gets smaller when b/h varies from 20 to 50; it is worth mentioning that the increasing in buckling load in case $(0/90/0)_S$ is more than other case where this increase reaches to10.81%.

5.2.4 Effect Number of Stiffeners:

From **Fig. 9,** it can be obtained that the buckling load increases with high percentage when the number of stiffeners increases because of the resistance of stiffener against load that causes buckling. Then, it is shown that in, SSSS, SFSF, the buckling load increases when number of stiffeners increases with percentage reaches to 57.988% and 81.619%respectively,increasing in buckling load in case SCSC is more than other case, it reaches to 59.94%.

5.2.5 Effect of stiffener depth ratio for stiffened plates:

It is shown from **Fig. 10,** the buckling loads decreases and increases with different percentage when d/h varies from 2 to 8 in all cases. It can be observed that the buckling load is decreased when d/h varies from2 to 4. Then, it is increased when d/h varies from 4 to 8; it is worth mentioning that the increasing in buckling load in case of plate with two stiffeners is more than other case where this increase reaches to17.733 %.Because of the number of stiffener and its resistance against load that causes buckling.

6. CONCLUSIONS

This study considers the buckling analysis of cross-ply composite laminate plate with various B.C's. From the present study, the following conclusions can be made:

1- The boundary conditions affect
   On the critical buckling load the maximum critical buckling load occurs at clamped boundary condition of plate. while the B.C's change from SSSS to SSCC ,the percentage of increasing the buckling load is (48.86%) for anti-symmetric cross under uniaxial load and the percentage of increasing buckling load when changing B.C's from SSFF to SSCC is (79.5%) for symmetric cross ply under uniaxial load.
2- The uniaxial buckling load decreases when a/b increase with high percentage reaches to 72.51% and 74.45% in SSSF and SFSF un-stiffened plate respectively. On the other hand in SCSC the buckling load decreases with small percentage reaches to 11.569% when a/b varies from 0.5 to 1.5, Then, it′s increases when a/b varies from 1.5 to 2. For un-stiffened plate under biaxial SFSS and SFSF, the buckling load decreases with high percentage when a/b increase reaches to 75.133% and77.129% in SFSS and SFSF respectively.
3- In unstiffened plate and plate with one stiffener the buckling load decreases when a/b increases with high percentage reaches to 67.383% and 57.878% in un stiffened plate and plate with one stiffener respectively.
4- The buckling loads increases when thickness ratio increases for un-stiffened plate under uniaxial or biaxial load. It can be observed that the buckling load is increase with high percentage when b/h varies from 10 to 20. Then, this percentage gets smaller when b/h varies from 20 to 50.
5- it can be obtained that the uniaxial buckling load increases with high percentage when the number of stiffeners increased , in SSSS, SFSF, the buckling load increase when number of

stiffeners increase with percentage reaches to 57.988% and 81.619 % respectively , increasing in buckling load in case SCSC is more than other case, it reaches to 59.94%.Then, for biaxial load SSSS, SCSC, the buckling load increase when number of stiffeners increase with small percentage reaches to 18.76 % and 18.91% in SSSS, SCSC, respectively , increasing in buckling load in case SCSC is more than other case, it reaches to 18.91%.

6- The buckling loads decreases and increases with different percentage when d/h varies from 2 to 8 in all cases for uniaxial load. It can be observed that the buckling load is decreased when d/h varies from2 to 4. Then, it is increase when d/h varies from 4 to 8; it is worth mentioning that the increasing in buckling load in case plate with two stiffeners is more than other case where this increase reaches to 17.733 %..

REFERENCES

- C. Guedes Soares and J.M.Gordo, 1997, *Design Methods for Stiffened Plates under Predominantly Uniaxial Compression,*Elsevier Science Limited, PII: S0951-8339(97)00002-6.

- Y.V.SatishKumar,Madhujit Mukhopadhyay, 1999, *A New Finite Element for Buckling Analysis of Laminated Stiffened Plates* Composite Structures, 46 (1999) 321-331.

- R.Rikards, A. Chate, O. Ozolinsh, 2001, *Analysis* for *Buckling And Vibrations Of Composite Stiffened Shells And Plates,* Composite Structures 51 (2001) 361-370.

- Samuel Kidane, 2002, *Buckling Analysis of Grid Stiffened Composite Structures.* M.Sc. thesis. Louisiana State University and Agricultural and Mechanical College.

- Aseel Jasim Mohammed Al-Hassani ,2005 *Instructional Model for Dynamic Analysis of Composite Plates Structure ,* PhD. Thesis Submitted to the University of Technology .

- W.Akl, A. El-Sabbagh, and A .Baz **,** 2008 *Optimization of The Static and Dynamic Characteristics of Plates with Isogrid Stiffeners, F*inite Elements in Analysis and Design 44 (2008) 513 – 523.

- Tran IchThinh, and Tran HuuQuoc, 2010, *Finite Element Modeling and Experimental Study on Bending and Vibration of Laminated Stiffened Glass Fiber/Polyester Composite Plates*, Computational Materials Science 49 (2010) S383–S389.

- Hasanain Ibrahim Nsaif**,** 2011 **,** *Buckling Analysis of Composite Plates under Thermal and Mechanical Loading*, M.sc, Thesis, University of Baghdad (2011)

- Reddy J.N. 2004 , *Mechanics of Laminated Composite Plates and Shells: Theory and Analysis*. 2ed; CRC Press 2004.

- M. S. Troitsky, D.Sc. 1976 , *Stiffened Plates Bending, Stability and Vibrations*, Elsevier Scientific Publishing Company (1976).

- Theory, analysis, and element manuals ANSYS 12.1 Program.

- Mei-Wen Guo, Issam E. Harik, Wei-XinRen, 2002, *Buckling Behavior of Stiffened Laminated Plates*, International Journal of Solids and Structures 39 (2002) 3039–3055.

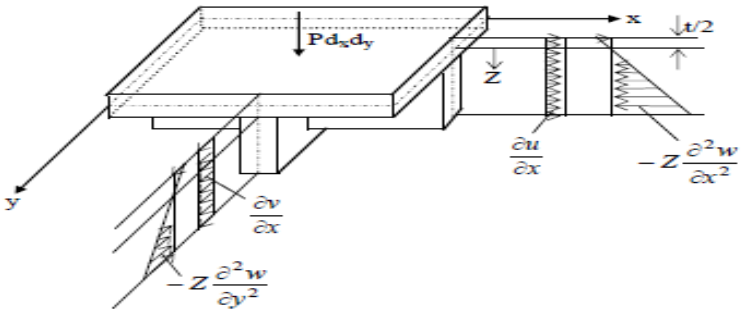

Figure 1: Distribution of normal strains for stiffened plates.

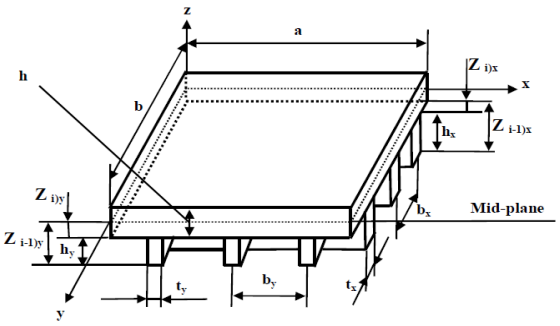

Figure 2: Dimensions and directions of stiffened laminated plates.

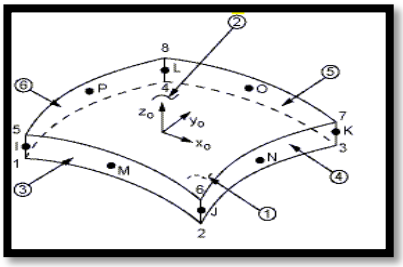

Figure 3: Shell281 Geometry [11]

Table 1. Dimensionless uniaxial buckling load $\bar{N}=N_{cr}\frac{a^2}{E_2h^3}$ of anti-symmetric cross ply laminates.

B.C'S	[9] Levy method	Present Levy method	(Discrepancy %)	E1/E2=40 G12=G13=0.6 E2 G23=0.5 E2 ν12=0.25 a=b h=1 N=10
S-F-S-F	6.78	6.796	(0.235%)	
S-F-S-S	7.05	7.417	(4.94%)	
S-F-S-C	8.221	8.276	(0.664%)	
S-S-S-S	12.109	12.722	(4.818%)	
S-S-S-C	12.607	12.86	(1.96%)	
S-C-S-C	13.254	13.41	(1.12%)	

Table (2) Dimensionless uniaxial buckling load $\bar{N}=N_{cr}\frac{a^2}{E_2h^3}$ of anti-symmetric cross ply laminates[$\mathbf{0^\circ/90^\circ/90^\circ/0^\circ}$] b/h = 10, G_{12}= G_{13}=0.6E_2, G_{23}=0.5E_2 , ν_{12}=0.25 , a=b , h=1.

E1/E2	[9]	ansys	discrepancy%
3	5.114	5.2556	2.77%
10	9.777	9.6985	0.80%
20	15.298	15.027	1.77%
30	19.957	19.405	2.76%
40	23.34	23.068	1.17%

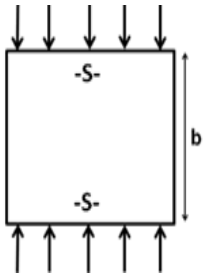

Table 3. Dimensionless uniaxial buckling load (λ) of anti-symmetric cross-ply laminated stiffened plate.$E_1 = 60.7GPa$,$E_2 = 24.8GPa$,$G_{12} = G_{31} = G_{23} = 12GPa$,$v_{12} = 0.23$
,$\lambda = {12N_{cr}a^2h(1-v^2)}/{E_1h^3}$, h=1, h/a=0.01, a=100, Stiffener Depth ratio (d/h) =4

a/b	Ref.[4]	Present F.E.M (**Discrepancy** %)	Present Levy Method (**Discrepancy** %)
0.5	54	52.84 (2.148%)	53.126 (1.61%)
1	75	74.66936 (0.44%)	72.865 (2.84%)
1.5	89	85.952 (3.048%)	87.357 (1.86%)
2	139	142.773 (2.7%)	140.236 (0.88%)

Table 4. Experimental mechanical properties of fiber glass-Polyester and young modulus for polyester.

Mechanical properties	Glass-polyester
E_1 (Mpa)	24800
E_2 (Mpa)	4485
G_{12} (Mpa)	1466
V_f	0.3

Figure 4. Buckling test machine.

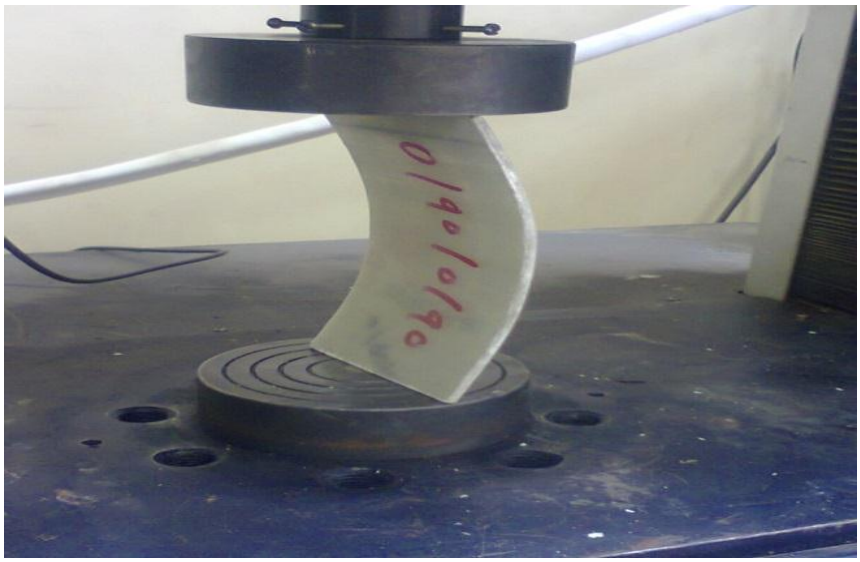

Figure 5a. Buckling test of S-F-S-F laminates without stiffener.

Figure 5b. Buckling test of S-F-S-F laminates with one stiffener.

Figure 5 c. Buckling test of S-F-S-F laminates with two stiffeners

Table 5. Dimensionless buckling load [$\bar{N} = N_{yy}^{0} * b^2/E_2 * h^3$] of SFSF laminates for un stiffened plate.

Laminated plate	Levy (Error %)	ANSYS (Error %)	Experimental
0/90	1.753 (3.57%)	1.712 (5.83%)	1.818
0/90/0	0.981 (1.3%)	0.972 (2.2213%)	0.994
0/90/0/90	2.487 (1.87%)	2.439 (3.77%)	2.5346
0/90/90/0	1.346 (3.925%)	1.285 (8.27%)	1.401

Table 6. Dimensionless buckling load [$\bar{N} = N_{yy}^{0} * b^2 / E_2 * h^2$] of SFSF laminates for stiffened plate

Number of stiffeners	Laminated plate	Levy (Error %)	ANSYS (Error %)	Experimental
One stiffener	0/90	11.923 (1.217%)	11.645 (3.52%)	12.07
	0/90/0	13.04 (1.762%)	12.249 (7.72%)	13.274
	0/90/0/90	29.53 (1.369%)	28.944 (3.326%)	29.94
	0/90/90/0	29.856 (1.747%)	29.26 (5.21%)	30.387
Two stiffeners	0/90	13.738 (2.608%)	13.334 (5.47%)	14.106
	0/90/0	15.127 (2.065%)	14.665 (5.05%)	15.446
	0/90/0/90	33.691 (1.044%)	33.337 (2.084%)	34.046
	0/90/90/0	43.752 (1.38%)	43.603 (1.719%)	44.366

Table 7. Effect of boundary condition on buckling load under uniaxial loading (0/90/90/0) with or without stiffeners.

Boundary condition	**Unstiffened plate**		**Plate with Single stiffener**		**Plate with two stiffeners**	
	Levy	ANSYS Error%	Levy	ANSYS Error%	Levy	ANSYS Error%
S-C-S-C	50.45	52.33 3.59%	245.23	247.5 0.91%	260.18	264.25 1.54 %
S-C-S-S	38.25	39.98 4.33%	242.53	245.1 1.07%	276.24	279.74 1.25 %
S-S-S-S	25.97	28.47 8.78%	218.24	220.6 1.09%	225.79	228.33 1.11%
S-F-S-C	11.56	12.29 5.91%	97.142	100.8 3.69%	126.34	131.25 3.73 %
S-F-S-S	2.45	2.59 5.4 %	114.97	118.2 2.76%	130.25	133.55 2.47%
S-F-S-F	1.25	1.28 2.34%	7.28	7.43 2.01%	13.176	14.544 9.40%

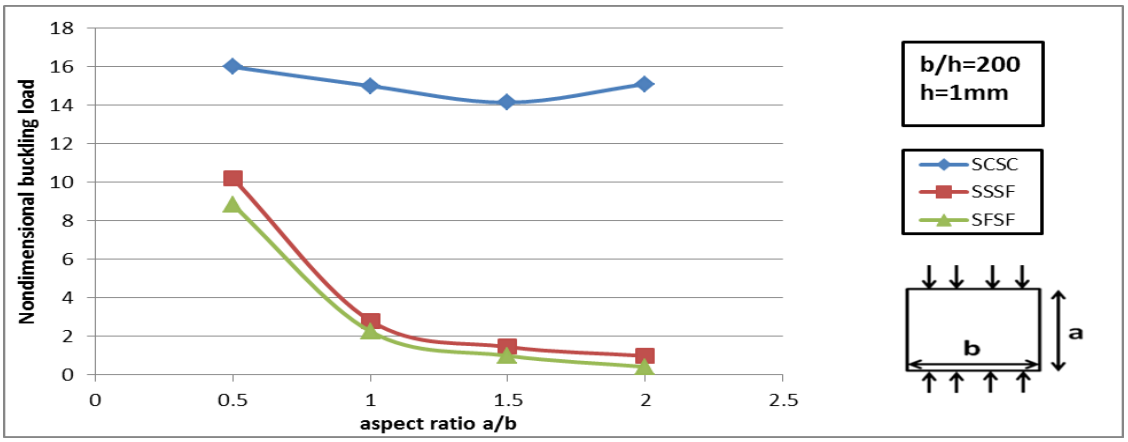

Figure 6. Non-dimensional buckling load(λ) versus aspect ratio (a/b) of anti-symmetric cross-ply (0/90/0/90) laminates under uniaxial compressive buckling load.

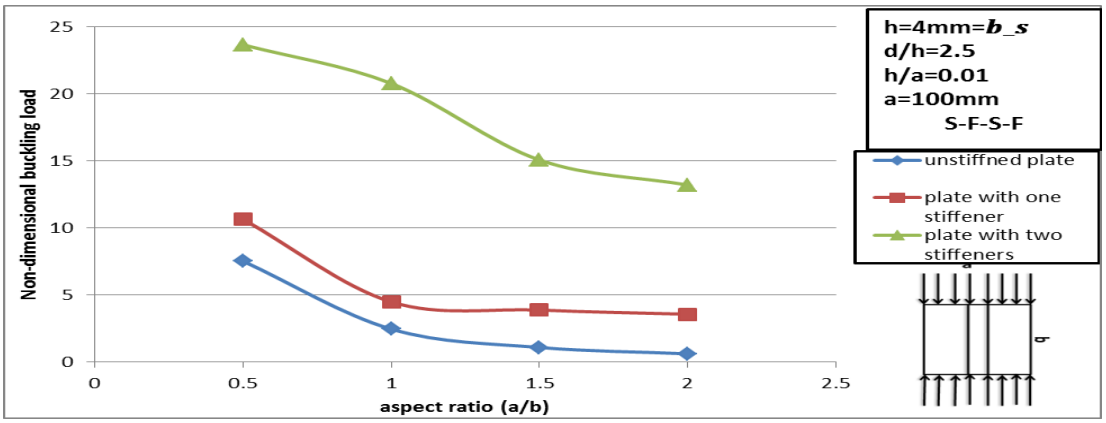

Figure 7 . Dimensionless uniaxial buckling load versus aspect ratio for stiffened and un stiffened plates.

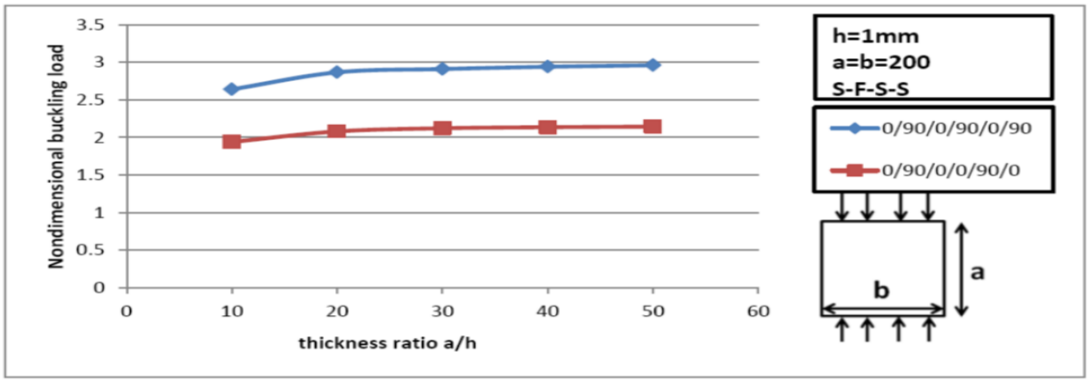

Figure 8. Non-dimensional buckling load(λ) versus thickness ratio, (a/h).

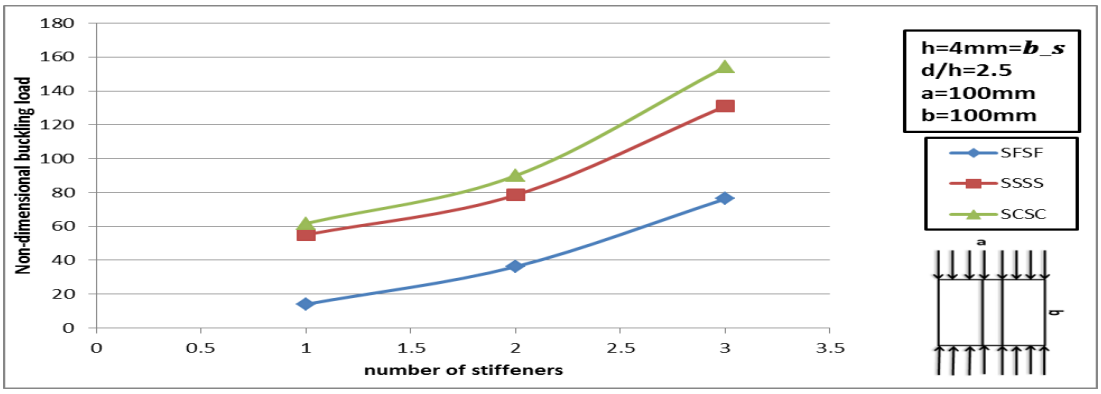

Figure 9. Dimensionless uniaxial buckling load versus No. of stiffeners of stiffened laminated plate.

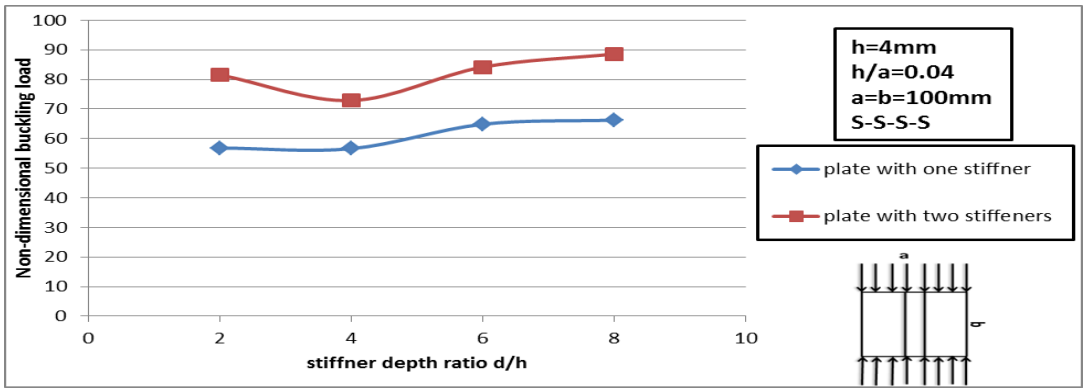

Figure 10. Dimensionless uniaxial buckling load versus stiffener depth ratio for stiffened plates.

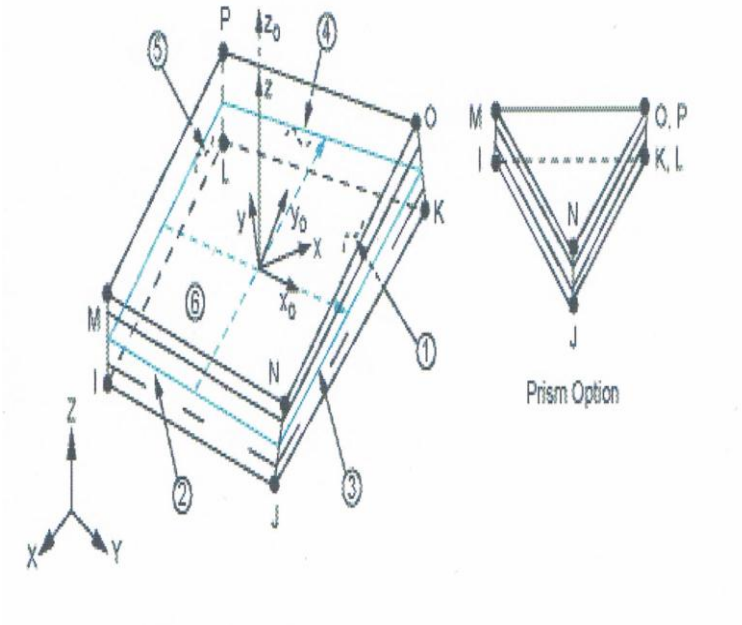

Figure 11. SOLSH190 Geometry [11].